

Interaction-assisted quantum tunneling of a Bose-Einstein condensate out of a single trapping well

Shreyas Potnis,^{1,*} Ramon Ramos,¹ Kenji Maeda,² Lincoln D. Carr,² and Aephraim M. Steinberg^{1,3}

¹*Centre for Quantum Information and Quantum Control and Institute for Optical Sciences, Department of Physics, University of Toronto, 60 St. George Street, Toronto, Ontario M5S 1A7, Canada*

²*Department of Physics, Colorado School of Mines, Golden, Colorado 80401, USA*

³*Canadian Institute For Advanced Research, 180 Dundas Street West, Toronto, Ontario M5G 1Z8, Canada*

(Dated: April 22, 2016)

We experimentally study tunneling of Bose-condensed ^{87}Rb atoms prepared in a quasi-bound state and observe a non-exponential decay caused by interatomic interactions. A combination of a magnetic quadrupole trap and a thin $1.3\mu\text{m}$ barrier created using a blue-detuned sheet of light is used to tailor traps with controllable depth and tunneling rate. The escape dynamics strongly depend on the mean-field energy, which gives rise to three distinct regimes—classical spilling over the barrier, quantum tunneling, and decay dominated by background losses. We show that the tunneling rate depends exponentially on the chemical potential. Our results show good agreement with numerical solutions of the 3D Gross-Pitaevskii equation.

The escape of a particle due to tunneling from a quasi-bound state is one of the earliest problems studied in quantum mechanics. When applied to understand α -decay of nuclei, it successfully explained not only the random nature of the decay, but also the large range of nuclear lifetimes, spanning many orders of magnitude [1]. Since then, quasibound states and quantum tunneling have been shown to play key roles in physical chemistry [2], biology [3], and condensed matter physics [4]. Consequently, tunneling has been studied in numerous systems, but mainly in those where the decay is irreversible and particles decay independently of one another, leading to the usual exponential dependence of the survival probability with time. In contrast to all these contexts, in this Letter we report non-exponential decay of a Bose-Einstein Condensate (BEC) from a quasibound state, arising due to interatomic interactions.

To obtain quasibound states of BECs, we developed a novel trapping geometry in which a thin repulsive optical barrier forms one of the walls of the trap, as depicted in Fig. 1. The ground state properties of the condensate in this trap show excellent agreement with mean-field theory. The strong exponential dependence of the tunneling rate on interactions is demonstrated by simultaneously measuring the number of atoms left in the trap and inferring the chemical potential from time-of-flight measurements of the condensate.

Techniques for preparing and manipulating ultra-cold atoms have matured in the past two decades, leading to a number of fundamental experiments on quantum tunneling. Experiments studying tunneling between bound states have explored Josephson oscillations and self trapping [5], the DC and AC Josephson effect [6], and the crossover from hydrodynamic and Josephson regimes [7]. In optical lattice systems, the interplay between inter-well tunneling and strong interactions is seen to give rise to the superfluid to Mott insulator transition [8, 9]. Meanwhile, experiments studying tunneling

from a bound state into the continuum are fewer, and largely study Landau-Zener tunneling out of an optical lattice. Early work on Landau-Zener tunneling of a BEC demonstrated inter-well coherence in the tunneling process by observing pulse trains emitted at the Bloch

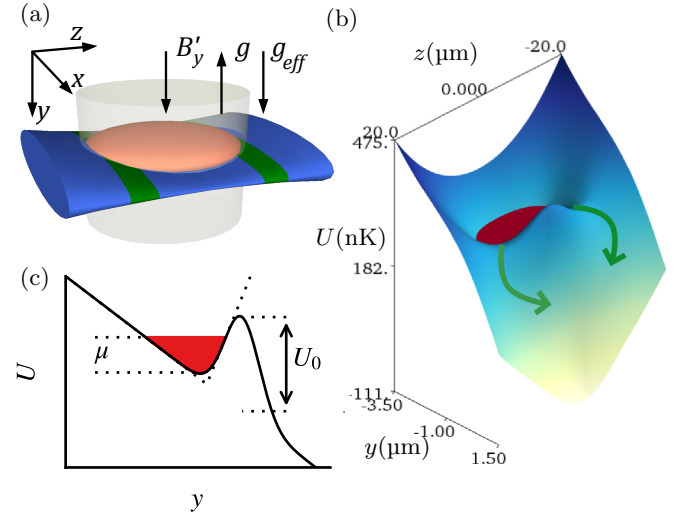


FIG. 1. Trap geometry for studying tunneling out of a quasibound state. (a) A blue-detuned light sheet propagating along the z direction forms one of the walls of the trap. Anti-Helmholtz coils provide a vertical field gradient B'_y which over-compensates gravity, resulting in a net acceleration g_{eff} along $+y$ and harmonic confinement in the x and z directions. The atoms are trapped in a small pocket created by the light sheet and the field gradient and tunnel towards $+y$ through two weak links indicated in green. (b) Surface plot of the potential energy U at $x = 0$. The tight focus of the barrier beam causes it to diffract out, increasing the barrier width off-center and decreasing the barrier height. The initial escape path through the two saddle points is indicated with green arrows. (c) A slice of the potential energy at $x = z = 0$ shown in solid black. A linear approximation, used to estimate the chemical potential, is indicated by the dotted lines.

frequency [10]. Since then, the role of interatomic interactions has been investigated in Landau-Zener tunneling [11, 12]. Deviations from an exponential decay have been demonstrated in Landau-Zener tunneling outside the BEC context, arising due to reversible system-environment coupling at early times [13], or due to Zeno and anti-Zeno effects [14]. However, in our work it is interactions and the statistical and macroscopic nature of BECs that create a highly non-exponential behavior.

While experiments have focused on tunneling between bound states, there has been much theoretical activity studying trapped ultra-cold gases tunneling into the continuum via a thin barrier. The effect of mean-field interactions on the tunneling rate has been calculated for both attractive and repulsive interactions, predicting a non-exponential decay curve [15]. Numerical simulations of dynamics of a trapped condensate tunneling out through a barrier reveal formations of shock waves inside the condensate, and blips emerging on the escaped side, as well as the formation of solitons [16, 17]. Studies of beyond-mean-field effects consider tunneling of a strongly interacting Tonks-Girardeau gas [18] and the development of correlations and fragmentation during the tunneling process [19]. Our work opens up the hitherto unexplored experimental regime of tunneling from a single trapping well into the continuum.

A central feature of our work is a novel Repulsive Sheet Trap (REST), formed using a combination of a quadrupole magnetic field and a blue detuned light sheet, as depicted in Fig. 1. The magnetic trap provides harmonic confinement in the horizontal directions with trapping frequencies $\omega_x = 2\pi \times 86$ Hz and $\omega_z = 2\pi \times 43$ Hz. Additionally, it provides a 28.3 G/cm vertical magnetic field gradient, which combined with gravity results in a net upward acceleration of $g_{\text{eff}} = 8.4 \text{ m/s}^2$. A thin light sheet serves as the tunnel barrier and is formed by focusing a 405 nm laser beam using a high Numerical Aperture (NA) objective (design based on Ref. [20]). The beam is nearly Gaussian with a waist $w_0 = 1.3(1) \mu\text{m}$ in the y direction and a Rayleigh range $z_R = 8 \mu\text{m}$, determined by knife-edge scans. An acousto-optic deflector is used to scan the beam in the x direction to create a flat potential within a 100 μm region [21].

Our experiment begins with a cloud of ^{87}Rb atoms in the $|F = 2, m_F = 2\rangle$ ground state evaporatively cooled close to degeneracy in a hybrid trap [22]. The magnetic field gradient is set to cancel gravity in the hybrid trap. The cloud is then adiabatically transferred to the REST trap by ramping up the barrier height U_0 and the magnetic field gradient while ramping down the power in the hybrid trap beam. Due to the small trapping volume of the REST trap, the phase space density increases during the transfer due to the dimple effect [23–25]. Further evaporation is achieved by lowering the barrier height to $\sim 550 \text{ nK}$ to get a pure BEC with 150k atoms. An RF knife is used transfer the escaped atoms to an untrapped

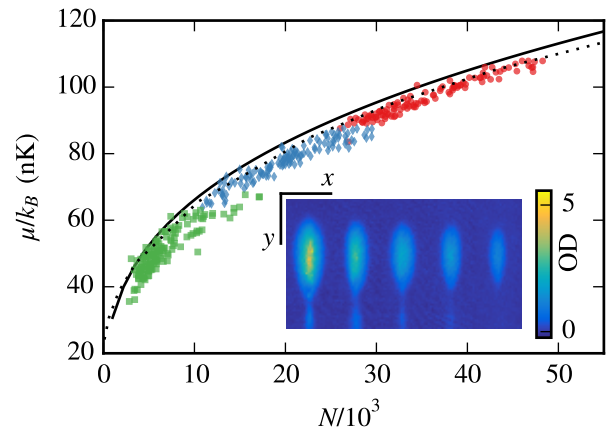


FIG. 2. The chemical potential μ of the condensate as a function of the number of atoms N for barrier heights of 330(35) nK (red circles), 290(30) nK (blue diamonds) and 240(25) nK (green squares). Black solid line is an estimate using Eq. 1 and the dotted line is a numerical solution of the 3D Gross-Pitaevskii Equation for a barrier height of 300 nK. The inset shows a collage of absorption images with progressively decreasing atom number from left to right. A trail of atoms spacing along the y direction is seen when the atom number is high. OD is the on-resonance optical density of the cloud after correcting for probe saturation effects.

m_F state and eject them out of the magnetic trap.

To initiate the tunneling dynamics, the barrier height is then non-adiabatically ramped down in 5 ms. The condensate is held in the trap for a variable time from 0.1 ms to 1.2 s. The trapping potentials are then abruptly turned off and the cloud is imaged after a 20 ms time-of-flight expansion. We image on the $F = 2 \rightarrow F = 3$ cycling transition using σ^+ light propagating along z and correct for probe saturation effects [26, 27] to ensure accurate atom number calibration. The atom number calibration is verified by measuring the critical temperature in the hybrid trap which agrees within 2% with the theoretically predicted value.

The expansion of the condensate during time of flight is highly anisotropic, as seen in the inset of Fig. 2. The tight confinement in the y direction causes the condensate to rapidly expand in the y direction, converting its interaction energy to kinetic energy [28, 29]. We extract the chemical potential from the final y width by fitting the 2D column density to an inverted paraboloid integrated along the imaging axis. This distribution, while strictly valid only for harmonic traps, fits our data well. Given our unusual trap geometry, there is no analytical expression for the chemical potential in the Thomas-Fermi limit. However, we can approximate the Gaussian barrier with a linear potential (see Fig. 1(c)) with an acceleration $a_b = 2U_0/mw_0\sqrt{e} - g_{\text{eff}}$ to get an analytical

approximation for the chemical potential:

$$\mu = \left\{ 12 (\hbar \bar{\omega})^2 (m \bar{a}) (N a_s) \right\}^{1/3}. \quad (1)$$

Here $\bar{\omega} = \sqrt{\omega_x \omega_z}$, N is the number of atoms, a_s is the s-wave scattering length, m is the mass of the particle and $\bar{a} = g_{\text{eff}} a_b / (g_{\text{eff}} + a_b)$ is the reduced acceleration.

Fig. 2 shows the chemical potential of the condensate for three different barrier heights. The barrier height U_0 is calculated by measuring the power in the barrier beam and calculating the AC Stark shift [30]. The reported uncertainty is due to systematic errors in estimating the transmitted fraction of the barrier beam through all the optics and due to uncertainty in the measured barrier waist. The chemical potential data agrees well with the approximation in Eq. 1, evaluated using measured trap parameters. However, due to the tight confinement in the y direction, we are in a regime where μ is comparable to the single particle ground state energy $\epsilon_0 = (\hbar m \bar{a}^2 / 2)^{1/3} \sim 20$ nK. Thus, kinetic energy corrections to the Thomas-Fermi approximation are important [31, 32]. Indeed, the agreement with data is better when the chemical potential is calculated by numerically solving the full 3D Gross-Pitaevskii Equation (GPE) equation, as seen in Fig. 2.

To characterize loss processes other than escape through the barrier, we study the decay from a trap with a high barrier height of 700 nK. At this barrier height, escape due to classical spilling and tunneling is negligible. We find that in the 1.5 s observation time, the decay is exponential with a decay rate of $\Gamma_{\text{bg}} = 0.31(2) \text{ s}^{-1}$, which we take as our background decay rate. This rate is consistent with the three-body recombination rate, given by $\Gamma_{\text{3b}} = L \langle n^2 \rangle$, where L is the three-body decay constant. For the REST trap in the Thomas-Fermi limit, we can show that $\langle n^2 \rangle = 3n_0^2/10 = (3/10) (\mu/g)^2$, where n_0 is the peak density. Using the value for L from Ref. [33] and the measured chemical potential $\mu = 92$ nK, we find that $\Gamma_{\text{3b}} = 0.34(9) \text{ s}^{-1}$. We do not find any discernible thermal component emerge during the hold. Thus, we can ignore losses due to heating and thermal activation.

Next, we discuss the escape dynamics of the condensate when the barrier height is lowered. Fig. 3 shows the number of atoms remaining in the trap with time on a semi-log plot. An exponential decay process, characterized by a constant decay rate, would appear as a straight line on a semi-log plot, whereas here we see a dramatic decrease in the decay rate with time. The decay rate $\Gamma = d \ln N / dt$, calculated by fitting sets of 5 consecutive points to a parabola and evaluating the slope at the center, is shown in Fig. 4(a).

We identify three distinct regimes in the decay process: (a) classical spilling over the barrier in the first 10-20 ms, (b) quantum tunneling from 20 ms to 0.5 s and (c) decay dominated by background losses from 500 ms

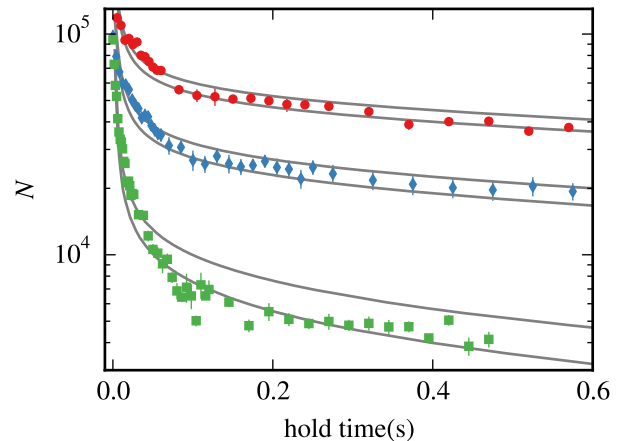


FIG. 3. Number of atoms N left in the trap after a hold time t for barrier heights of 330(35) nK (red circles), 290(30) nK (blue diamonds) and 240(25) nK (green squares). Solid gray lines are results of 3D GPE simulations for a barrier height of 230, 240, 290, 300, 340 and 350 nK from bottom to top. Only the first 0.6 s are shown here since the decay rate approaches the background decay rate at later times.

onward. The initial non-adiabatic lowering of the barrier height causes the condensate to rapidly expand and spill over the two saddle points of the trap, as shown in Fig 1(b). The 5 ms initial ramp-down time of the barrier height is chosen to be comparable to $1/\omega_z = 3.7$ ms, so that it is slow enough not to cause sloshing in the trap after the ramp down, but fast enough that tunneling does not begin as the barrier is being ramped down. We expect the spill to occur on a similar timescale, and indeed we see that in the first 10-20 ms, μ drops to below the trap depth U_s , at which point the decay transitions from classical spill to quantum tunneling.

The trap depth U_s , which is the difference in potential energy at the saddle point and the bottom of the trap, is calculated from the peak barrier height U_0 and measured trap parameters. In Fig. 4(a), the points where the chemical potential is greater than U_s are shown in gray. Close to the transition point where $\mu \sim U_s$, the Γ vs μ data shows a kink and the decay rate starts dropping exponentially after the transition. This provides confirmation that the decay mechanism has switched from classical spilling to tunneling. The tunneling regime is characterized by an exponential dependence of the decay rate on the chemical potential. There is a small range of μ of about 20 nK for which the tunneling range is appreciable. In this range the decay rate Γ drops dramatically until it reaches the background decay rate.

The experimental results are compared against full 3D GPE simulations, with measured trap parameters and initial atom numbers used in the simulations. The ground state is first found by imaginary time propaga-

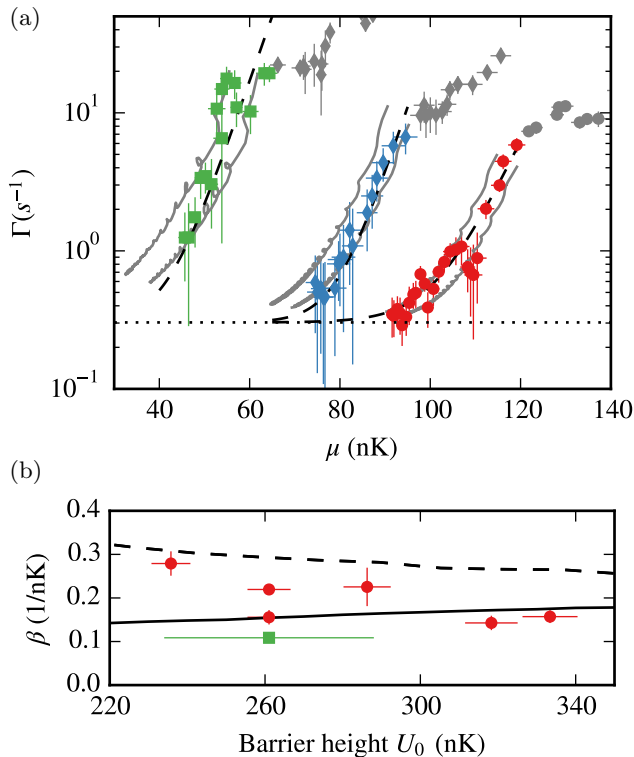


FIG. 4. (a) Decay rate Γ as a function of the chemical potential μ . Horizontal dotted line indicates the background decay rate. Data points where the chemical potential is greater than the trap depth U_s are shown in gray. The dashed line is a fit to the function $\Gamma = \Gamma_{\text{bg}} + \exp(\alpha + \beta\mu)$ and solid gray lines are results of 3D GPE simulations. Data points shown in gray are not used for fitting, and correspond to classical spilling. The color schemes match those shown in Fig. 3. (b) The slope β as a function of barrier height. Vertical error bars are obtained from the fit. Horizontal error bars represent statistical fluctuations in the barrier power, except for the green square, which represents the systematic error. Solid and dashed lines are results of 3D GPE simulations 1D single particle transfer matrix calculations respectively.

tion in a trap with a high barrier height. Mimicking the experiment, the barrier height is then lowered using a linear ramp to a final value. Absorbing boundary conditions were added to avoid reflections of the escaped atoms from the edge of the grid. The strength of the absorber smoothly increases with distance from the barrier to avoid reflections from the absorber. From Fig. 3 and Fig. 4, we see that our data agrees well with the simulations. Oscillations in the chemical potential curves in Fig. 4 are due to breathing mode oscillations surviving after the initial spill out. The small disagreement of our data with simulations could be attributed to a systematic error in estimating the barrier height and the slight non-Gaussian nature of the barrier beam due to residual spherical aberrations in the focused beam. Fig. 4b compares the slope β of the $\log(\Gamma) - \mu$ curves against results

results of both 3D GPE simulations and a 1D transfer matrix calculation with a barrier height U_s and width equal to the waist size at the saddle point of the potential. A WKB-style argument suggests an exponential dependence on μ , where the steepness depends primarily on the barrier thickness. Here we see that both the single-particle and GPE simulations give exponential behavior, with slopes between 0.15 and 0.3 nK^{-1} , consistent with our data.

In conclusion, using a novel trapping configuration, we have demonstrated for the first time quantum tunneling of a condensate from a single trapping well into the continuum, and shown the exponential dependence of the tunneling rate on the chemical potential. Having shown good agreement with mean-field simulations, our trapping geometry may be extended to observe tunneling of many-body states. For low atom numbers of around 100-1000, μ would be comparable to ϵ_0 , which freezes out all the dynamics in the vertical (y) direction, making the condensate two dimensional. By further confining the atoms by scanning the barrier beam in both the x and y directions in a U-shaped pattern, even create one-dimensional condensates could be created. Tunneling dynamics of 1D or 2D condensates, where phase fluctuations and defects have been seen [34, 35], would be an intriguing future direction of research[36]. Tunneling out of the REST trap occurs through two symmetric points, and the tunneled atoms recombine at a time $\pi/2\omega_z$. The contrast of the resulting interference pattern could be used as a probe of the coherence of tunneled atoms, and fragmentation of the condensate [19]. Studies of manifestly quantum phenomenon such as tunneling of macroscopic systems like these can be used to test the validity of quantum mechanics at the macroscopic level, and investigate the crossover from the quantum to classical [37].

The authors thank Rockson Chang, David Spierings, Diego Alcala and Xinxin Zhao for helpful discussions and A. Stummer for technical support. Computations were performed on the gpc supercomputer at the SciNet HPC Consortium [38]. SciNet is funded by the Canada Foundation for Innovation under the auspices of Compute Canada; the Government of Ontario; Ontario Research Fund - Research Excellence; and the University of Toronto. Finally, we acknowledge support from NSERC, CIFAR, NSF, ASOFR and Northrop Grumman Aerospace Systems.

* spotnis@physics.utoronto.ca

- [1] R. W. Gurney and E. U. Condon, *Physical Review* **33**, 127 (1929).
- [2] D. Gatteschi and R. Sessoli, *Angewandte Chemie International Edition* **42**, 268 (2003).
- [3] E. Collini, C. Y. Wong, K. E. Wilk, P. M. G. Curmi,

- P. Brumer, and G. D. Scholes, *Nature* **463**, 644 (2010).
- [4] H. J. Choi, J. Ihm, S. G. Louie, and M. L. Cohen, *Phys. Rev. Lett.* **84**, 2917 (2000).
- [5] M. Albiez, R. Gati, J. Fölling, S. Hunsmann, M. Cristiani, and M. K. Oberthaler, *Phys. Rev. Lett.* **95**, 10402 (2005).
- [6] S. Levy, E. Lahoud, I. Shomroni, and J. Steinhauer, *Nature* **449**, 579 (2007).
- [7] L. J. LeBlanc, A. B. Bardou, J. McKeever, M. H. T. Extavour, D. Jervis, J. H. Thywissen, F. Piazza, and A. Smerzi, *Physical Review Letters* **106**, 025302 (2011).
- [8] M. Greiner, O. Mandel, T. Esslinger, T. W. Hänsch, and I. Bloch, *Nature* **415**, 39 (2002).
- [9] R. Jördens, N. Strohmaier, K. Günter, H. Moritz, and T. Esslinger, *Nature* **455**, 204 (2008).
- [10] B. P. Anderson, *Science* **282**, 1686 (1998).
- [11] O. Morsch, J. H. Müller, M. Cristiani, D. Ciampini, and E. Arimondo, *Physical Review Letters* **87**, 140402 (2001).
- [12] M. Cristiani, O. Morsch, J. H. Müller, D. Ciampini, and E. Arimondo, *Phys. Rev. A* **65**, 63612 (2002).
- [13] S. R. Wilkinson, C. F. Bharucha, M. C. Fischer, K. W. Madison, P. R. Morrow, Q. Niu, B. Sundaram, and M. G. Raizen, *Phys. Rev. Lett.* **77**, 5315 (1996).
- [14] M. C. Fischer, B. Gutiérrez-Medina, and M. G. Raizen, *Physical review letters* **87**, 040402 (2001).
- [15] L. D. Carr, M. J. Holland, and B. A. Malomed, *Journal of Physics B: Atomic, Molecular and Optical Physics* **38**, 3217 (2005).
- [16] G. Dekel, V. Farberovich, V. Fleurov, and A. Soffer, *Physical Review A* **81**, 063638 (2010).
- [17] L. Salasnich, A. Parola, and L. Reatto, *Phys. Rev. A* **64**, 23601 (2001).
- [18] A. del Campo, F. Delgado, G. García-Calderón, J. G. Muga, and M. G. Raizen, *Physical Review A* **74**, 013605 (2006).
- [19] A. U. J. Lode, A. I. Streltsov, K. Sakmann, O. E. Alon, and L. S. Cederbaum, *Proceedings of the National Academy of Sciences of the United States of America* **109**, 13521 (2012).
- [20] W. Alt, *Optik - International Journal for Light and Electron Optics* **113**, 142 (2002).
- [21] R. Chang, S. Potnis, C. W. Ellenor, M. Siercke, A. Hayat, and A. M. Steinberg, *Phys. Rev. A* **88**, 53634 (2013).
- [22] R. Chang, S. Potnis, R. Ramos, C. Zhuang, M. Hallaji, A. Hayat, F. Duque-Gomez, J. E. Sipe, and A. M. Steinberg, *Phys. Rev. Lett.* **112**, 170404 (2014).
- [23] P. W. H. Pinkse, A. Mosk, M. Weidemüller, M. W. Reynolds, T. W. Hijmans, and J. T. M. Walraven, *Physical Review Letters* **78**, 990 (1997).
- [24] D. M. Stamper-Kurn, H.-J. Miesner, A. P. Chikkatur, S. Inouye, J. Stenger, and W. Ketterle, *Physical Review Letters* **81**, 2194 (1998).
- [25] Y.-J. Lin, A. R. Perry, R. L. Compton, I. B. Spielman, and J. V. Porto, *Phys. Rev. A* **79**, 63631 (2009).
- [26] G. Reinaudi, T. Lahaye, Z. Wang, and D. Guéry-Odelin, *Optics Letters* **32**, 3143 (2007).
- [27] M. Egorov, *Coherence and collective oscillations of a two-component Bose-Einstein condensate*, Ph.D. thesis, Centre for Atom Optics and Ultrafast Spectroscopy Swinburne University of Technology, Melbourne, Australia. (2012).
- [28] G. Baym and C. J. Pethick, *Physical Review Letters* **76**, 6 (1996).
- [29] Y. Castin and R. Dum, *Phys. Rev. Lett.* **77**, 5315 (1996).
- [30] R. Grimm, M. Weidemüller, and Y. B. Ovchinnikov, *Advances in atomic, molecular, and optical physics* **42**, 95 (2000).
- [31] E. Lundh, C. J. Pethick, and H. Smith, *Physical Review A* **55**, 2126 (1997).
- [32] A. M. n. Mateo and V. Delgado, *Physical Review A* **75**, 063610 (2007).
- [33] J. Söding, D. Guéry-Odelin, P. Desbiolles, F. Chevy, H. Inamori, and J. Dalibard, *Applied Physics B* **69**, 257 (2014).
- [34] S. Richard, F. Gerbier, J. H. Thywissen, M. Hugbart, P. Bouyer, and A. Aspect, *Physical Review Letters* **91**, 010405 (2003).
- [35] S. Stock, Z. Hadzibabic, B. Battelier, M. Cheneau, and J. Dalibard, *Physical Review Letters* **95**, 190403 (2005).
- [36] J. A. Glick and L. D. Carr, *arXiv:1105.5164*.
- [37] A. J. Leggett, *Progress of Theoretical Physics Supplement* **69**, 80 (1980).
- [38] C. Loken, D. Gruner, L. Groer, R. Peltier, N. Bunn, M. Craig, T. Henriques, J. Dempsey, C.-H. Yu, J. Chen, L. J. Dursi, J. Chong, S. Northrup, J. Pinto, N. Knecht, and R. V. Zon, *Journal of Physics: Conference Series* **256**, 012026 (2010).